

# Development of methods for determining the tracking software systems accuracy, application of a wireless communication device and self-contained power supply in heliostat units with centralized monitoring and control system

**F A Satybaldiyeva<sup>1\*</sup>, D Beyer<sup>2</sup>, A S Sarybaev<sup>3</sup>**

<sup>1</sup>Kazakh National Research Technical University named after K.I.Satpayev

<sup>2</sup>University of Applied Sciences Schmalkalden

<sup>3</sup>M. Auezov South Kazakhstan State University

\*Corresponding author's e-mail: feruza201200@gmail.com

Received 20 March 2017, www.cmnt.lv

## Abstract

This article deals with determination of accuracy in tracking software systems, and advantages of the heliostat automatic control system that utilizes measuring informational and control systems comprising wireless measuring instruments and information-processing equipment. The heliostat automatic control system covered in the article is one of the types of measuring informational and control systems. As distinct from other measuring informational systems, the described heliostat control system operates only when tracking parameters deviate towards the maximum permitted values.

Use of wireless communication between detectors, transducers and industrial logical controllers in modern optical SPS heliostat control systems is more advantageous than laying hundreds meters of cable.

To provide power supply, it is proposed to equip each heliostat with a self-contained power supply, since heliostat operates when concentrated solar radiation in the receiver is sufficient for steam generation, while the rest of the time it is in the standby mode. That is why use of a solar battery-powered self-contained power supply is more advantageous than use of centralized power supply from the industrial network.

## Keywords

mathematical model, automatic control systems, heliostat, wireless communication, power supply

## 1 Introduction

The objective of accuracy determination in tracking software systems (TSS), just as in optical tracking systems (OTS), is to determine the misalignment angle between the Sun and the optical axis in concentrators or the set direction of reflection in heliostats.

In OTS, this angle is directly recorded by an optical detector (OD) that sends the signal for misalignment angle handling, with OTS also performing drive errors and rotational axes positions compensation due to available feedback. That is, when tracking using OTS, there are practically no requirements for drive errors and rotational axes positions. TSS operates as follows. The control program calculates the Sun's angular position in a coordinate system associated with a concentrator (or heliostat) — the Sun's angular coordinates are determined, based on which the software determines the angles of heliostat turning (the angles of concentrator turning are equal to the Sun's angular coordinates in one CS), the drives receive a signal for handling of these angles. That is, TSS cannot “see” the Sun, and thus there is no compensation of drive errors and rotational axes and, accordingly, control algorithm errors. But here we also obviously need control of concentrator turning angles, i.e. feedback is required as well. This task was considered and solved in the course of

development of the Big Solar Furnace (BSF) heliostat software control system; the azimuthal and zenithal drive reducers were equipped with angular sensors at a pitch of about 36 arcsec. These sensors controlled the angles of heliostat turning in terms of azimuth and zenith. Field research of the sensors operation was performed. The experimental design was as follows: heliostat was put into the tracking mode using an optical sensor, while turning angles were determined by an angular sensor and further compared in time with the designed angles of turning. Assessment of actual angle deviations of heliostat turning angles in terms of azimuth and zenith against their designed values was carried out on the basis of the data obtained. It was established that difference between the angles does not exceed 1-2 arcmin, and the conclusion was made that it proves accuracy of the software tracking. It was also stated, that the BSF heliostat tracking systems operate practically in the on-off mode: “start-stop-start”. It should be noted that characteristics of the misalignment angle sensor itself (angular value of dead spot) were not investigated.

## 2 Theory and calculations

As is known, solar cell concentrators (heliostats) must turn (keep track) of the Sun with a certain level of accuracy due to its apparent movement.

At that, along with concentrator's accuracy

characteristics, tracking accuracy is one of the factors influencing the solar radiation concentration, i.e. irradiance variation in the focus and mean concentrations at the receiver. Tracking accuracy, as was determined above, is clearly defined by a defocusing angle  $\beta$  or by an angular deviation of axial solar beams from either optical axis of the concentrator (the concentrator mode) or predetermined direction of solar beam reflection from the heliostat (the heliostat mode). At the initial approximation, the defocusing leads to a shift of a concentrated spot at the receiver. The methodical task setting (concepts of static and dynamic defocusing modes), as well as experimental and calculation studies of the influence of defocusing, virtually the only ones to the present day, were conducted in [2-5]. In these studies, allowed values for defocusing angles  $\beta$  were identified for energy concentrators. It was found that  $\beta$  must not exceed 16 arcmin at the acceptable flow reduction at the receiver by 10% for concentrators of solar power plants. The issue of permissible defocusing angles also becomes relevant due to problems of development of software systems for concentrators (heliostats) to keep track of the Sun. Acceptable values of defocusing angles obtained in [2-5] generally allow to make the conclusion on possible requirements for the tracking accuracy, although during the design of tracking systems it is still assumed that the tracking accuracy must not exceed 1 arcmin.

Flow densities at the receiver's surface elements and subsequently flows will be determined using the model suggested by Grilikhes V.A. [1]. This model assumes that even if beams are reflected from a non-precise concentrator, the angular dimension of the reflected solar cone will not change; and that concentrator inaccuracies are distributed according to some randomly set rule with the standard angular deviation  $\sigma$  of normals in relation to normals of a precise concentrator. In practice, this integral is defined numerically and actually is replaced by a sum of the following type. For example, when determining the flow on the area  $S_R$  of the receiver, it will be as follows:

$$E_A = \sum_{S_R} dS \sum_{S_C} B(\mathbf{a}) * (\mathbf{n}_M * \mathbf{a}) * (\mathbf{n}_A * \mathbf{a}) * d\omega, \quad (1)$$

where  $B(\mathbf{a})$  is the brightness of the reflected solar beam from the  $M$  point (the surface element of the concentrator in the direction of  $A$  point of the receiver (the unit vector  $\mathbf{a}$ );  $\mathbf{n}_M$  and  $\mathbf{n}_A$  are  $M$  and  $A$  area normals;  $d\omega$  is the elementary solid angle with a vertex in the  $A$  point;  $S_R, S_C$  are surface areas of the receiver and the concentrator.

As stated in [2], the surface area of the concentrator  $S_C$  and its geometry, specular reflection factor ( $R_c$ ), coordinates of  $M$  and  $A$  points, orientation of normal  $\mathbf{n}_A$  in the center of the receiver's surface element  $dS_A$ , and incident irradiation parameters (for the Sun, it is usually a vector direction of the axial solar beam  $\mathbf{c}$ , its angular radius  $\varphi_0$  and the angular distribution of brightness  $f(\varphi, \varphi_0)$  across the solar disk) shall be set in order to determine components of the irradiance integral. Based on these formulas, we developed an algorithm as well as software in C++ for calculation of both

the irradiance and the flow from a paraboloid concentrator based on a flat receiver surface, taking into account the possibility to set the concentrator inaccuracies and the defocusing angle in the software.

The following sun spot radius  $r_p$  of the precise paraboloid will be used as the size scale, as well as for the purpose of results summarization [3]:

$$r_p = p * \varphi_0 / [(1 + \cos U_0) * \cos U_0], \quad (2)$$

where  $p$  is the focal paraboloid parameter ( $p = 2f$ ,  $f$  is focal length);  $\varphi_0$  is the angular radius of the solar disk;  $U_0$  is concentrator's opening angle valid for a circular concentrator and effective for other shapes [4].

Overall influence of the defocusing angle  $\beta$  on irradiance distribution in the focal plane of a precise paraboloid concentrator ( $\sigma = 0$ ) on a concentrated spot is shown in Fig. 1, where for comparison you may also see irradiance distribution for a non-precise concentrator ( $\sigma = 8$  arcmin) for the case of  $\beta = 0$ . As we can see, assumptions in [1, 10] were confirmed, as sufficiently large defocusing angles mainly resulted in the shifting of spot leaving the irradiance curve's shape unchanged.

Fig. 1 shows that due to the uneven distribution of a concentrated spot, the influence of defocusing may vary for receivers of different radii (different average concentration).

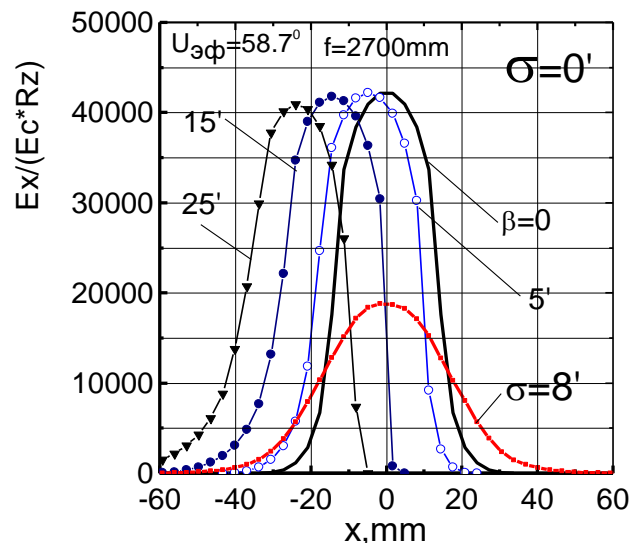


FIGURE 1 Irradiance distribution in the focal plane of a precise parabolic concentrator in the cross-section  $y=0.05r_p$  ( $r_p = 31$  mm) at different defocusing angles  $\beta$ .

Thus, the following typical dimensions of the spot radii may be identified for the given concentrator with  $U_0 = 58.7^\circ$  for the area radius  $r$  in fractions of the image spot radius of the precise concentrator  $r_p$ : I – the focal up to  $r/r_p \approx 0.05$ , where  $C \approx 42,324$  (at  $\sigma = 0$ ) and  $C \approx 18,800$  (at  $\sigma = 8$ ); II – the area of high mean concentration, up to  $r/r_p \approx 0.25$  where  $C \approx 40,440$  ( $\sigma = 0$ ) and  $C \approx 18,100$  ( $\sigma = 8$ ); III – the border of sharp drop of the irradiance curve, up to  $r/r_p \approx 0.35$  where  $C \approx 38,600$  at  $\sigma = 0$ , while for the non-precise concentrator, it is up to  $r/r_p \approx 0.7$  where  $C \approx 12,200$  ( $\sigma = 8$ ); IV – the border of a sloping part and the irradiance curve, the radius of which for

a precise concentrator is equal to  $r/r_p \approx 0.65$  and  $C \approx 20,500$  ( $\sigma = 0$ ), while for a non-precise concentrator it is  $r/r_p \approx 1$  and  $C \approx 8000$  ( $\sigma = 8$ ). That is, even in the case of the non-precise paraboloid concentrator, the average concentrations are quite high within the spot. Moreover, which is important in practice, for the non-precise concentrator the main flow falls into the spot area of the precise concentrator, i.e. in the area of  $r/r_p \approx 1$ .

For the same concentrator Fig. 1 illustrates flow changes at these areas depending on the angle of defocusing  $\beta$  for both precise ( $\sigma = 0$ ) and non-precise ( $\sigma = 8'$ ) concentrators. To sum up the results,  $F_\beta$  flows at the receiver are shown in a relative form, as the fractions of flow incident on this area in the absence of defocusing  $F_{\beta=0}$ , i.e. when  $\beta=0$ . To allow determination of the  $F_{\beta=0}$  flow fraction in the total flow, there are also  $F_{\beta=0}$  values given in fractions of the total flow  $F_p$  [5] reflected from the concentrator.

Due to the fact that the flow change depending on  $\beta$  is quite minor, requirements for tracking inaccuracy  $\alpha_c$  and its impact on reduction of flow  $\Delta F/F_{\beta=0} = (1-F_\beta/F_{\beta=0}) * 100\%$  for the practical case — the non-precise concentrator with  $\sigma = 8'$  — are presented in a tabular form (Table 1). Here we may clearly see the actual difference between the defocusing angle and tracking inaccuracies or the misalignment angle. Thus, in fact, to ensure the required defocusing angle, it is necessary that actuation angles  $\alpha_a$  and  $\alpha_h$  or projections of misalignment angle  $\alpha$  at  $\alpha_a = \alpha_h$  in the sensor planes were:

$$\alpha_a = \alpha_h = 0.7\alpha.. \tag{3}$$

TABLE 1 Flow reduction ( $\Delta F/F_{\beta=0}$ , %) at the receiver of  $r/r_p$  radius, depending on the misalignment angle  $\alpha_c$  and tracking inaccuracy  $\alpha_a = \alpha_h$  for a non-precise concentrator ( $\sigma = 8'$ ).

| $\alpha_c = \beta$<br>arcmin | $\alpha_a = \alpha_h$ ,<br>arcmin | area radius, $r/r_p$   |      |      |       |
|------------------------------|-----------------------------------|--|------|------|-------|
|                              |                                   | 0.05   | 0.25 | 0.7  | 1.0   |
|                              |                                   | $\Delta F / F_{\beta=0} = (1 - F_\beta / F_{\beta=0}) * 100\%$ |      |      |       |
| 0                            | 0                                 | 0  | 0    | 0    | 0     |
| 1                            | 0.7                               | 0  | -0.1 | -0.1 | -0.03 |
| 2                            | 1.4                               | 0.6  | 0.1  | 0.1  | 0.08  |
| 3                            | 2.1                               | 0.6  | 0.7  | 0.6  | 0.3   |
| 4                            | 2.8                               | 0.8  | 1.5  | 1.2  | 0.8   |
| 5                            | 3.5                               | 1.4  | 2.7  | 2.2  | 1.3   |
| 6                            | 4.2                               | 2.8  | 4.2  | 3.4  | 1.9   |
| 7                            | 4.9                               | 4.6  | 5.9  | 4.8  | 2.8   |
| 8                            | 5.6                               | 7  | 8.0  | 6.5  | 3.7   |
| 9                            | 6.3                               | 8.8  | 10.0 | 8.3  | 4.8   |
| 10                           | 7                                 | 12   | 13   | 10.4 | 6.0   |

As Table 1 shows, in the case of tracking inaccuracy  $\alpha_c = 2'$  ( $\alpha_a = \alpha_h = 1.4'$ ), almost no reduction of flow and, consequently, concentration  $C$  occurs, and reduction of about 1% only occurs when  $\alpha_c = 4'$  ( $\alpha_a = \alpha_h = 2.8'$ ). Thus, tracking accuracy may be at the level of  $4'$  ( $\alpha_a = \alpha_h = 2.8'$ ) for solar furnaces, while for solar power plants tracking inaccuracy may be up to  $7'$  ( $\alpha_a = \alpha_h = 4.9'$ ) for the cases where the receiver radii ( $r/r_p$ ) are at the level of 0.7-1 with acceptable flow reduction of 3%.

Having determined the software tracking accuracy in the Lab View virtual environment, we considered the model of application of a wireless communication device and self-contained power supply in heliostat units with centralized monitoring and control system [7, 11, 12].

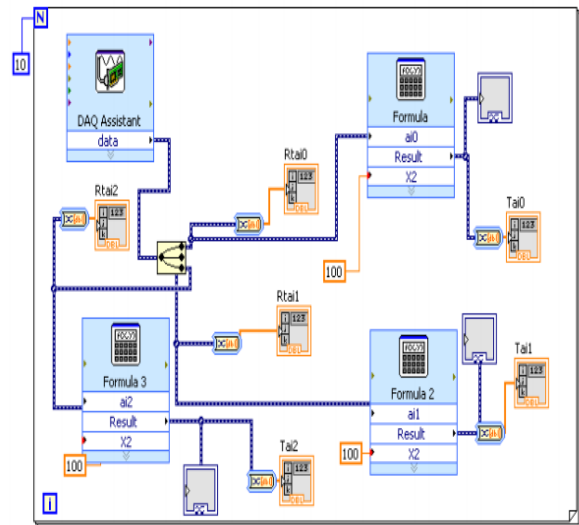


FIGURE 2 Creates a window of the diagram in Lab View

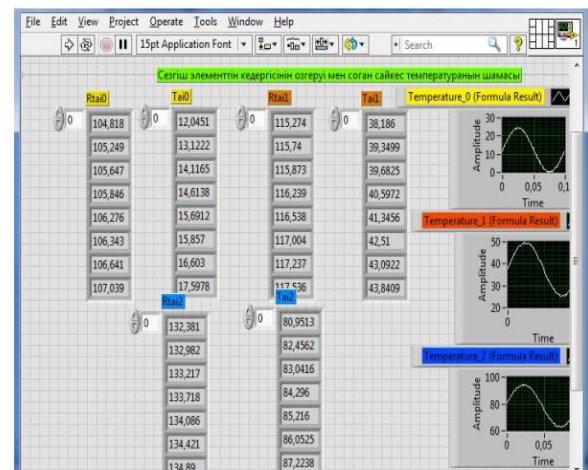


FIGURE 3 Meteorological parameters in LabView format opened with graphics editor National Instruments LabView

### 3 Experimental materials and methods

Currently, three types of heliostat automation systems are used, i.e.:

- the individual automatic control system;
- the centralized monitoring and control system;
- the combined monitoring and control system.

The operation concept of the individual automatic control system is that each heliostat operates individually, independently of each other, and each of them is equipped with tracking, positioning and orientation devices.

The centralized automation system monitors and controls the whole heliostat field from the operator's room.

The combined automation control system includes both of the above control systems [3, 17].

Let us consider the centralized control system for solar power station (SPS) automation. In addition to individual heliostat control system devices, the centralized control system includes centralized control devices with functions of feedback and control of each heliostat's orientation.

When controlling the SPS heliostat field, the control commands (certain codes of analog or digital signals) are sequentially transferred in a group or separately to each heliostat individually: start of operation, movement, stop, end of operation and reset. Control commands (electric signals) are transferred to heliostats via signal cables while power is transferred via power cables. The precise control of a corresponding heliostat is achieved by introduction of a specific system of signal coding and receiver addressing.

Accuracy of heliostat control will be mainly determined by accuracy of automatic control system operation.

Figure 4 presents a block diagram of a centralized automatic monitoring and control system, which performs control from the primary system by means of continuous signals or impulses sent at specific time intervals according to the Sun's position on the dome of the sky. At that, the control commands must be generated (formed) in the primary control system.

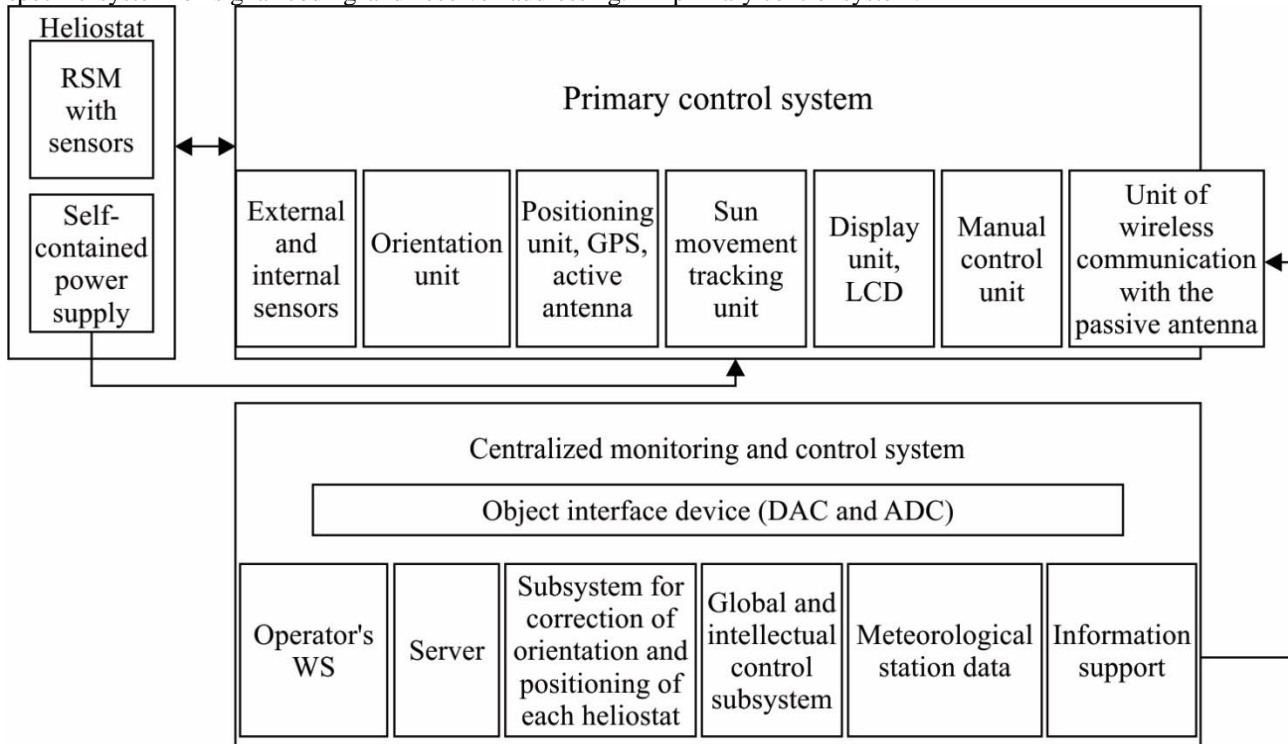


FIGURE 4 Centralized monitoring and control system

In case of use of the above automated control system (ACS) scheme with optical SPSs, each heliostat must be equipped with two electric drives with appropriate reduction gears to ensure zenithal and azimuthal turning and with four position sensors for precise pointing (on each heliostat) [1,8].

The considered automatic heliostat control system is one of types of measuring informational and control systems, which are complexes of measuring instruments and information-processing equipment. Their characteristic feature is that they are designed to obtain information on operating parameters values, which are characterized by the "pointed" or "misaligned" states, directly from the controlled (monitored) object. That is why such control systems must be functionally linked with the controlled object and must receive information directly from the object (from heliostat groups).

The matter of remote information transmission, i.e. communication channels, is of special importance for automated control systems on optical SPSs with a great number of heliostats.

The automatic control unit for all heliostats of an optical SPS system deals with signals transmitting information over a distance via wires (communication channels) [11, 14]. Their main objectives are communication effectiveness and reliability, i.e. transmission of the greatest volume of information using the most economical way with the least

distortion caused by various disturbances introduced by the communication channels themselves or due to other reasons.

For sequential control of turning of separate heliostat groups, the control signals must be transmitted via the communication channel in a specific sequence. This function may be performed by a multichannel system with time distribution of the channels. When building multichannel systems, the values of controlled variables are usually represented by a uniform parameter, such as DC voltage, resistance, etc. To transmit values via a communication channel, the uniform parameter is converted to an intermediate parameter, which ensures the least errors caused by instability of communication channel parameters or disturbances. At the receiving point, the intermediate parameter is converted to direct current or other signals allowing to register the values of controlled variables or reproduce them.

#### 4 Results and analysis

Thus, analysis of design, technical parameters of heliostats on operating tower-type SPSs, as well as analysis of the composition, functions and operation of automation systems allow us to make the following conclusions [5, 9, 15]:

- land area utilization efficiency is not high, as heliostats are bulky and, accordingly, the area

- occupied by a heliostat field is very large;
- the cost of a heliostat with the reflective surface area of 50 m<sup>2</sup>, a tower with height of 80 m or more, equipped with a tracking system, position sensors, electronic positioning and orientation devices is relatively high;
- large overall dimensions and weight of heliostats complicate their control in terms of accuracy of sun rays pointing to a receiver (free play, deformation, etc.);
- due to the weight of mirrors, frame, rotary support mechanisms (RSM) and pillar of heliostat with reflective surface area of 50 m<sup>2</sup>, the power consumption increases to 200 W/h;
- periodic switching on and off of motors of rotary support mechanisms is carried out by powerful, large, noncontact and contact electronic and electric power elements;
- electrical communication, signal transmission and exchange with heliostat's electronic devices and the automation system are carried out in the analog form, using a signal cable network;
- coordination of the industrial computer with controlled objects requires a great amount of DAC and ADC inputs and outputs;

- high power consumption by automation devices and the monitoring and control system.

In an optical system of tower-type SPS, the communication with the upper level of the automation system is carried out via a signal cable network. Heliostat power supply is arranged via a power cable network. Power and signal cables are laid in special ducts, trays and trenches. Currently, costs of cables and their laying are rather high, and they comprise 10% of the SPS's total cost.

With development of network and telecommunications technologies, wireless communication between detectors, transducers and industrial logical controllers is widely used in modern SCADAs. These devices are small and may be embedded directly into primary automation facilities. These devices are cheap and their application is more advantageous than laying hundreds meters of cable. That is why, to reduce costs and expenses on purchase and laying of signal cables, we propose to use cheap but effective wireless devices. Figure 5 below presents a schematic diagram of a receiver-transmitter developed by MikroElektronika on the basis of nRF24L01P microcircuit. As we can see, the diagram is simple, the additional elements connected to the microcircuit are required only for setting of its operating parameters.

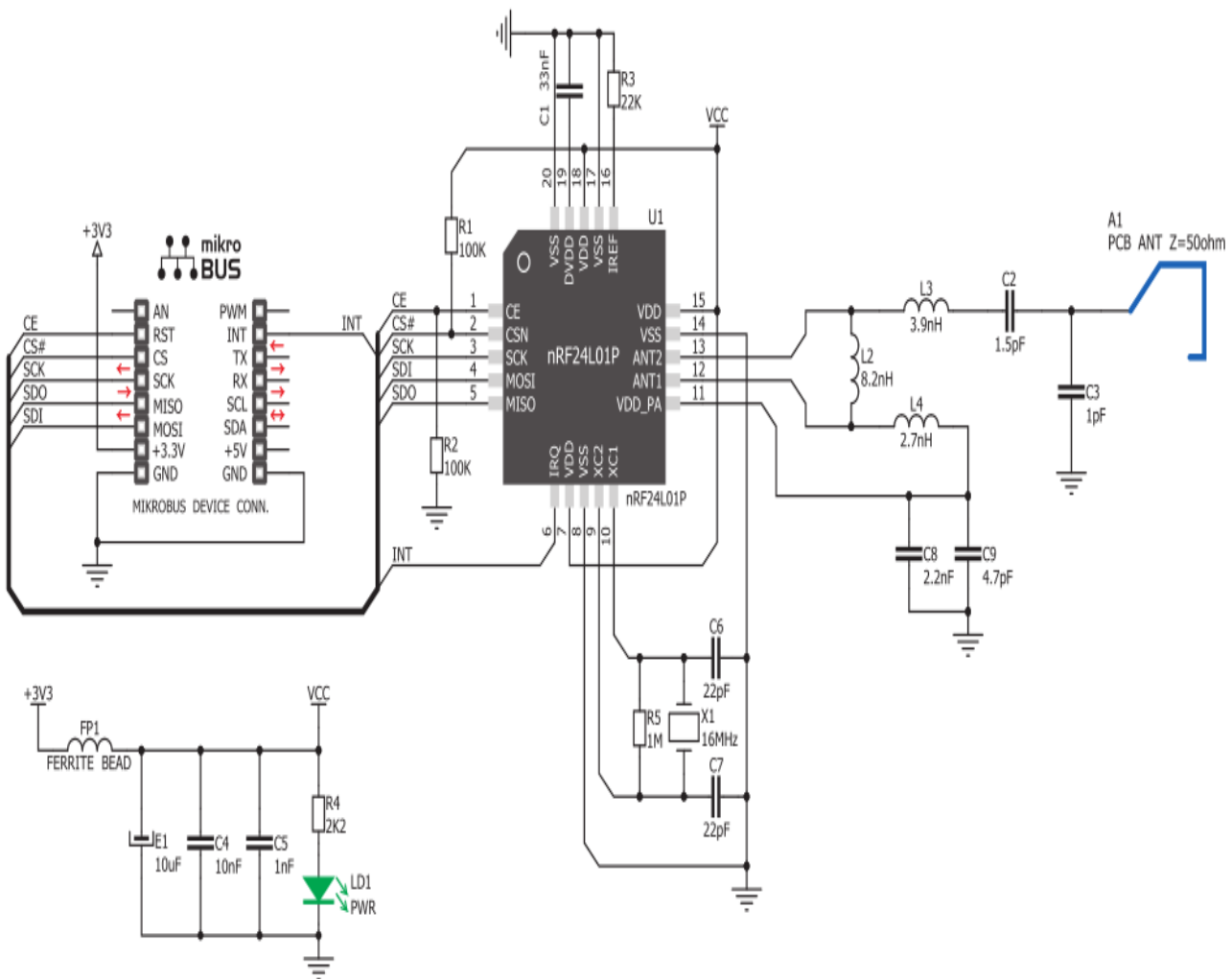


FIGURE 5 Schematic diagram of wireless device

This device can transmit both analog and discrete signals over a distance of up to two kilometers. The transmit and receive speed is 10 Mbit/s, the transmitter's operating frequency is 2.8 mHz, power supply is 5 V. The heliostat is equipped with RSM, electronic RSU motor control unit and wireless receiver and transmitter. To provide them with DC power, we propose to equip every heliostat with a self-contained power supply [11, 12, 15].

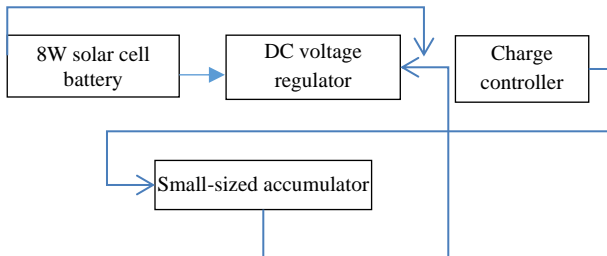


FIGURE 6 Block diagram of self-contained DC power supply composition

This power source (PS) consists of the following units presented in Figure 6.

This PS is cheap and small-sized. The solar panel is installed directly on the heliostat's reflecting surface. Heliostat operates only in weather when concentrated solar radiation in the receiver is sufficient for steam generation, while the rest of the time it is in the standby mode [15]. That is why use of a solar battery-powered self-contained power supply in our opinion is more advantageous than use of centralized power supply from the industrial network. It should be noted that this self-contained PS is designed to supply several adjacent small-sized heliostats, see Figure 7.

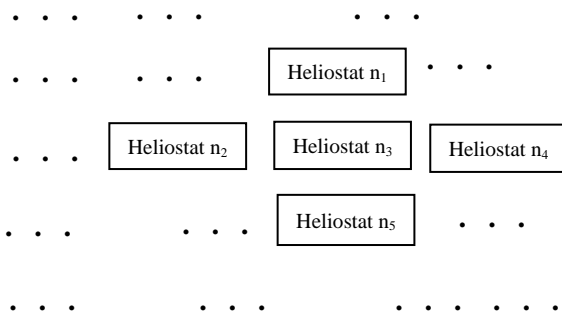


FIGURE 7 Heliostat field

References

[1] Abdurahmanov A A, Orlov S A, Bakhranov S A, Bourbeau A V, Klychev I, Fazil H K 2010 On the accuracy of tracking the sun concentrators *Solar technology* 4 82-5  
 [2] U. Thein Lin 2009 *Stepper motor control system for moving the frame of the solar power plant. Natural and Technical Sciences*. M.: "The company Sputnik +" 1 292-5  
 [3] Sarybaev S A, Satybaldiyeva F A, Sarybay M A, Kultas A K 2014 Principles of controlling the orientation of the solar solar plants *Almaty Herald KBTU* 3(30) 80-4  
 [4] Sarybaev A 2006 *Research and development of an automated control system of heliostats to extend the functionality of a large solar furnace capacity of 100kV* Abstract of Cand. Ph.D. T.: 25  
 [5] Klychev S I 2002 Simulation of optical-power characteristics of solar radiation concentrators *Solar technology* 3 59-63

For the purpose of saving the energy generated by the self-contained PS, control of n-group of heliostats and i-th heliostat in the n-group is carried out sequentially. For example, a self-contained PS provides power to five heliostats (Figure 7.). All the electronic control devices of the five heliostats are connected to the self-contained PS, but all RSM motors are disconnected from PS, and each RSM motor  $n_i$  sequentially connects to PS when performing functions of pointing, manual control, reset after maintenance or repair, setting to the next morning position and specific positioning in the period of extreme weather conditions. Thus, the monitoring and control methods fundamentally change when using a self-contained PS.

5 Conclusions

Tracking inaccuracy calculations and available conclusions given us the 15% efficiency factor based on the defined general relation between the defocusing angle  $\beta$  and misalignment angle  $\alpha$  in measuring planes of the optical tracking sensor. [19] It was shown that for cases of both concentrator and heliostat modes of tracking,  $\alpha$  is always equal to  $\beta$ , although the nature of their changing as well as their projections may vary, and that in practice the actual tracking inaccuracy in the sensor planes must not exceed  $\alpha_a = \alpha_h \leq 0.7\beta$  [16].

Common link between the defocusing angle  $\beta$  and misalignment angle  $\alpha$  in measuring planes of the tracking optic sensor has been determined, we demonstrated that  $\alpha = \beta$  always, both in the concentrator and in the heliostat tracking mode, though the nature of their variation and their projections may differ, and in practice the actual tracking inaccuracy in sensor planes must not exceed  $\alpha_a = \alpha_h \leq 0.7\beta$ .

As distinct from other measuring informational systems, the described heliostat control system operates only when tracking parameters deviate towards the maximum permitted values. Thus, the considered diagram provides a much simpler way of comparing the obtained parameters against the preset parameters.

Acknowledgements

We would like to express a gratitude to reviewers for valuable comments.

*Bulletin of the Kazakh Academy of Sciences Almaty* 5 188-98

- [10] Zahidov R A 1986 *Mirror concentration of radiant energy system T: "FAN"* 173
- [11] Ismailov S U, Satybaldiyeva F A, Beysembekova R N, Saribaev A S, Musabekov A A, Ismailov A S 2016 Electronic circuit based on pic microcontroller for heliostat departments with a support rotating mechanism for tracking the sun *Reports of the national academy of sciences of the republic of kazakhstan* 3
- [12] Archer B 1980 Comments on "Calculating the position of the sun" *Solar Energy* 25 91
- [13] Joseph J 1988 Michalsky The Astronomical Almanac's Algorithm For Approximate Solar Position (1950-2050) *Solar Energy* 40(3) 227-35
- [14] Sarybaev A S, Beysembekova R N, Ismailov S U 2016 Development and research optimization system power output of thermal reactors by changing the orientation solar installations *The International Conference on Energy and Infrastructure Management (ICEIM-2016)*, *School Of Petroleum Management Pandit Deendayal Petroleum University Gandhinagar- 382007, Gujarat, India* 31-40
- [15] AlFaify S, Rammah Y S, Zahran H Y, Yakuphanoglu F, Mohd. Shkir 2016 Optical Properties of Nano-Rods PTCDA Thin Films: an Important Material for Optoelectronic Applications *Natural Sciences Publishing (NSP) OrganoOpto-Electronics (OOE)* 2
- [16] Yurchenko A V, Kozlov A V 2007 The long-term prediction of silicon solar batteries functioning for any geographical conditions *Proceedings of 22st European PV Solar Energy Conference and Exhibition. Milan 3-7 September 3019-22*
- [17] Aipov P C, Yarmukhametov W R 2007 Improving the efficiency of solar power plants *Mechanization and electrification of SH* 9 29-30
- [18] Witzke A, Kaluza N J 2001 Test of Device Accelerated Ageing of Polymeric Material in High Concentrated Sunlight at the DLR Solar Furnace *5th Cologne Solar Symposium* 152-8

| AUTHORS   |   |
|---|---|
|    | <p><b>Satybaldiyeva Feruza</b></p> <p><b>Current position, grades:</b> PhD student of Kazakh National Technical University.</p> <p><b>University studies:</b> Master degree in computer engineering and software from International University of Information Technologies.</p> <p><b>Scientific interests:</b> Optical tracking sensor</p> <p><b>Publications:</b></p> <ol style="list-style-type: none"> <li>Development and research optimization system power output of thermal reactors by changing the orientation solar installations. The International Conference on Energy and Infrastructure Management (ICEIM-2016). SCHOOL OF PETROLEUM MANAGEMENT PANDIT DEENDAYAL PETROLEUM UNIVERSITY GANDHINAGAR- 382007, GUJARAT, INDIA 2016, c. 31-40</li> <li>Creation of control over the orientation of the solar systems helio concentration. INTERNATIONAL SCIENTIFIC AND PRACTICAL CONFERENCE Kyrgyz State University named I.Arabaeva 2015, pp 200-203</li> <li>Software Development of an automated control system experimental solar №5. 2014 Bulletin of the Kazakh Academy of Sciences Almaty 2014 pp.188-198</li> </ol> <p><b>Experience:</b> Experience in software development and process automation.</p> |
|   | <p><b>Ditmur Beyer</b></p> <p><b>Current position, grades:</b> professor University of Applied Sciences Schmalkalden</p>  |
|  | <p><b>Sarybaev Abdushukur</b></p> <p><b>Current position, grades:</b> senior lecturer, Candidate of Technical Sciences South Kazakhstan National University after named M. Auezov</p>   |